Bi-Allelic *UQCRFS1* Variants Are Associated with Mitochondrial Complex III Deficiency, Cardiomyopathy, and *Alopecia Totalis*

Mirjana Gusic,[1,2,12] Gudrun Schottmann,[3,4,12] René G. Feichtinger,[5,12] Chen Du,[6] Caroline Scholz,[6] Matias Wagner,[1,2,7] Johannes A. Mayr,[5] Chae-Young Lee,[3,4] Vicente A. Yépez,[8] Norbert Lorenz,[9] Susanne Morales-Gonzalez,[3,4] Daan M. Panneman,[10] Agnès Rötig,[11] Richard J.T. Rodenburg,[10] Saskia B. Wortmann,[1,2,5] Holger Prokisch,[1,2] and Markus Schuelke[3,4,*]

Isolated complex III (CIII) deficiencies are among the least frequently diagnosed mitochondrial disorders. Clinical symptoms range from isolated myopathy to severe multi-systemic disorders with early death and disability. To date, we know of pathogenic variants in genes encoding five out of 10 subunits and five out of 13 assembly factors of CIII. Here we describe rare bi-allelic variants in the gene of a catalytic subunit of CIII, *UQCRFS1,* which encodes the Rieske iron-sulfur protein, in two unrelated individuals. Affected children presented with low CIII activity in fibroblasts, lactic acidosis, fetal bradycardia, hypertrophic cardiomyopathy, and *alopecia totalis*. Studies in proband-derived fibroblasts showed a deleterious effect of the variants on UQCRFS1 protein abundance, mitochondrial import, CIII assembly, and cellular respiration. Complementation studies via lentiviral transduction and overexpression of wild-type *UQCRFS1* restored mitochondrial function and rescued the cellular phenotype, confirming *UQCRFS1* variants as causative for CIII deficiency. We demonstrate that mutations in *UQCRFS1* can cause mitochondrial disease, and our results thereby expand the clinical and mutational spectrum of CIII deficiencies.

Complex III (CIII, also called ubiquinol:cytochrome *c* oxidoreductase or bc1 complex) is an electron transfer enzyme complex; it is the component of the mitochondrial respiratory chain that transports electrons from ubiquinol to cytochrome *c*. This redox reaction is coupled to proton translocation from the mitochondrial matrix to the intermembrane space via the "Q-cycle," contributing to the proton gradient required for ATP synthesis.[1] Mammalian CIII possesses a symmetrical dimeric structure ($CIII_2$) in which each monomer is composed of 10 different subunits.[2–4] Three of those subunits are catalytic and possess electron transfer properties: CYB, CYC1, and UQCRFS1, whose intermembrane-space-facing C terminus contains an iron-sulfur (2Fe-2S) cluster. UQCRFS1 is synthesized as a pre-protein in the cytosol, and its import into the mitochondrial matrix is directed by its cleavable N-terminal mitochondrial targeting sequence (MTS). Following import, UQCRFS1 is stabilized by the chaperone LYRM7.[5,6] Direct binding of the co-chaperone HSC20 to LYRM7 is required for recruitment of the 2Fe-2S transfer complex to the LYRM7-UQCRFS1 intermediate, and ultimately for 2Fe-2S cluster incorporation into UQCRFS1.[7] Once UQCRFS1 has acquired its 2Fe-2S cluster, BCS1L translocates and incorporates it into the pre-$CIII_2$ complex, rendering it catalytically active.[8,9] Interestingly, cleavage of the UQCRFS1 MTS is carried out only after its incorporation into $CIII_2$.[7] Although crystal structures from bovine heart CIII revealed the presence of UQCRFS1 N-terminal-derived peptides in between the core subunits UQCRC1 and UQCRC2,[2,9,10] later research showed that their prominent accumulation in the absence of TTC19 would be detrimental to CIII function.[11] Hence the current assumption is that during its incorporation, UQCRFS1 is processed *in situ,* and several peptides containing its MTS remain bound to $CIII_2$. Later, these peptides have to be removed to preserve $CIII_2$ structural integrity and function. This process is facilitated by TTC19.[9,11] The functional importance of this turnover still needs to be elucidated, especially in the context of different metabolic demands.[9] Within the mitochondrial respiratory chain, $CIII_2$ is forming supercomplexes together with Complex I (CI) and Complex IV (CIV), and the most abundant of these supercomplexes ($CI_1III_2IV_1$) is termed "respirasome."[12–14]

Isolated CIII deficiencies are among the least frequently diagnosed mitochondrial disorders. They are associated with heterogeneous clinical presentations.[15–17] To date, mutations in genes encoding five subunits, *MT-CYB*

[1]Institute of Human Genetics, Helmholtz Zentrum München, 85764 Neuherberg, Germany; [2]Institute of Human Genetics, Technical University Munich, 81675 Munich, Germany; [3]Charité-Universitätsmedizin Berlin, corporate member of the Freie Universität Berlin and Humboldt-Universität zu Berlin, and Berlin Institute of Health: NeuroCure Cluster of Excellence, 10117 Berlin, Germany; [4]Charité-Universitätsmedizin Berlin, corporate member of the Freie Universität Berlin and Humboldt-Universität zu Berlin, and Berlin Institute of Health: Department of Neuropediatrics, 13353 Berlin, Germany; [5]University Children's Hospital, Salzburger Landeskliniken (SALK) and Paracelsus Medical University (PMU), 5020 Salzburg, Austria; [6]Institute of Human Genetics, Medizinische Hochschule Hannover, 30625 Hannover, Germany; [7]Institute of Neurogenomics, Helmholtz Zentrum München, 85764 Neuherberg, Germany; [8]Department of Informatics, Technical University of Munich, 81371 Garching, Germany; [9]Department of Pediatric Cardiology, Municipal Hospital Dresden, 01307 Dresden, Germany; [10]Radboud Center for Mitochondrial Disorders, Department of Pediatrics, Radboud UMC, Nijmegen 6525, the Netherlands; [11]UMR 1163, Université Paris Descartes, Sorbonne Paris Cité, Institut IMAGINE, 24 Boulevard du Montparnasse, 75015 Paris, France
[12]These authors contributed equally to this work
*Correspondence: markus.schuelke@charite.de
https://doi.org/10.1016/j.ajhg.2019.12.005.

Table 1. Clinical Phenotypes of Both Probands Encoded According to the Human Phenotype Ontology (HPO)

Characteristics and Symptoms	HPO ID	Proband 1	Proband 2
Mutation in *UQCRFS1* (NM_006003)	NA	homozygous c.215-1G>C	c.41T>A | c.610C>T
Effect on translation (NP_005994)	NA	p.Val72_Thr81del10	p.Val14Asp | p.Arg204*
Origin	NA	Afghanistan	Germany
Gender	NA	male	male
Age at onset	NA	congenital	congenital
Age at last assessment	NA	3.5 months	9 years
Age at death	NA	3.5 months	NA
Fetal Development			
Intrauterine growth retardation (<P10)	HP:0001511	-	+
Low birth weight	HP:0001518	- (59th percentile)	+ (3rd percentile)
Fetal bradycardia	HP:0001662	+	+
Perinatal Development			
Persistent fetal circulation	HP:0011726	ND	+
Hypothermia	HP:0002045	+	ND
Feeding difficulties	HP:0008872	+	+
Hyperventilation	HP:0002883	+	ND
Metabolism			
Lactic acidosis [highest level]	HP:0003128	24 mmol/l	15 mmol/l
Metabolic crises during febrile infections	HP:0004897	ND	+
Cardiovascular System			
Hypertrophic cardiomyopathy	HP:0001639	+	+
Ventricular septal defect	HP:0001629	-	+
Persistent left superior *vena cava*	HP:0005301	-	+
Pericardial effusion	HP:0001698	+	ND
Motor System			
Muscular hypotonia	HP:0001252	(+)	+
Muscular weakness	HP:0001324	+	+
Delayed motor development	HP:0001270	ND	+
Elevated creatine kinase levels [highest]	HP:0003236	>5,000 U/l	ND
Hematologic System			
Thrombocytopenia	HP:0001873	(+)	+
Normochromic anemia	HP:0001895	ND	+
Abnormality of blood coagulation	HP:0001928	+	ND
Visual System			
Bilateral papilledema	HP:0001085	ND	+
Skin and Appendages			
Alopecia totalis	HP:0007418	+	+
Gastrointestinal System			
Cholelithiasis	HP:0001081	+	ND

NA—not applicable, ND—not done or no information available

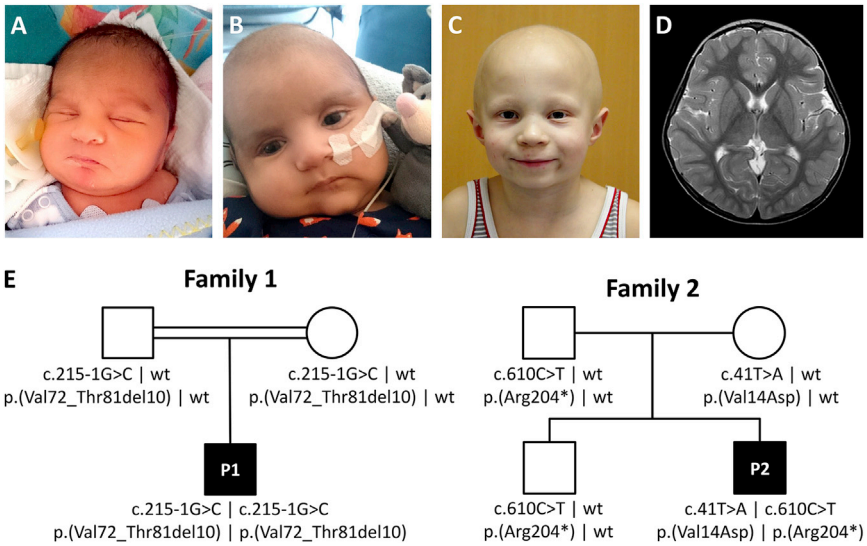

Figure 1. Clinical Images of Both Probands and Family Pedigrees
(A and B) Proband 1 (P1) at the age of 1 week (A) and of 8 weeks (B) after loss of his scalp hair.
(C) Proband 2 (P2) at the age of 6 years with *alopecia totalis* of his scalp with only sparse hair growing around his eyebrows.
(D) Entirely normal cranial MRI scan of P2 without characteristic T_2-signal-intense areas in the basal ganglia; these areas are often seen in Leigh syndrome and many other mitochondrial disorders.
(E) Pedigrees of both families with *UQCRFS1* genotypes.

(MIM: 516020),[18,19] *CYC1* (MIM: 615453),[20] *UQCRC2* (MIM: 191329),[21] *UQCRB* (MIM: 19330),[22] and *UQCRQ* (MIM: 612080),[23] and five assembly factors, *UQCC2* (MIM: 614461),[24,25] *UQCC3* (MIM: 616097),[26] *LYRM7* (MIM: 615838),[6] *BCS1L* (MIM: 124000, 603358, and 262000),[27–29] and *TTC19* (MIM: 615157),[30] have been reported in more than 140 individuals.[25]

With more than 50 published cases, the most frequent causes of CIII deficiency are variants in *MT-CYB,* typically associated with myopathy and exercise intolerance. This is followed by more than 30 cases with variants in *BCS1L* that are associated with either Björnstad syndrome or GRACILE syndrome.[17,25] Both of these syndromes are severe neurologic and multi-systemic diseases with neonatal onset. Similar phenotypes have been reported in individuals with pathogenic variants in *UQCRB*, *UQCRC2,* and *CYC1*, who presented with neonatal or early infantile onset, recurrent metabolic crises with elevated lactate levels and hypoglycemia, from which they completely and quickly recovered with intravenous glucose. All but one showed normal development and intellect.[25] Based solely on clinical presentation, it is impossible to distinguish between subunit or assembly factor defects. All reported affected individuals are following an autosomal recessive mode of inheritance, apart from those with pathogenic variants in the mitochondrial DNA (mtDNA)-encoded *MT-CYB* that are maternally inherited or occur spontaneously. CIII defects, with the exception of TTC19 deficiency, often present as combined respiratory chain deficiencies in combination with CI and, in some cases, with CIV deficiencies.[24,31] One reason could be the formation of supercomplexes, in which the presence of fully assembled CIII would be a prerequisite for the stability or assembly of CI and CIV.[25,32]

In this study, we report the clinical and molecular findings of two unrelated children with CIII deficiency, lactic acidosis, fetal bradycardia, lactic acidosis, hypertrophic cardiomyopathy, and *alopecia totalis* (Table 1). We recruited both individuals from the German network for mitochondrial disorders (MitoNET). Their parents provided written informed consent for all aspects of the study and for publication of facial photographs according to the Declaration of Helsinki. The ethical committees of both participating centers (Charité EA2/107/14 and TU Munich 5360/12S) have approved the study.

The male proband 1 (P1, Figure 1) was the first child of consanguineous Afghan parents, born at term by emergency *Caesarean* section due to fetal bradycardia. At the first day of life, physicians noted hypothermia, borderline thrombocytopenia (152/nL; N > 150), lactic acidosis (24 mmol/l; N < 2.0), and elevated creatine kinase levels (>5.000 IU/l; N < 190). Skin and skeletal muscle biopsies were performed on the first day of life. Measurements of respiratory chain enzyme activities showed normal values in the muscle and low-normal values in skin fibroblasts for combined CII+III activity (Tables S1 and S2). Metabolic urine tests revealed increased excretion of ketone bodies and of lactate. Plasma alanine was markedly elevated. Thiamine and coenzyme Q_{10} supplementation was initiated. Electroencephalogram (EEG) showed slightly pathologic baseline activity initially, but EEG results were normal at 7 weeks of age. Neonatal screening revealed hearing impairment. Echocardiography at the first day of life showed septum and right ventricle hypertrophy, increased right-ventricular pressure (≈65% of systemic pressure), and a patent *ductus arteriosus* with bi-directional shunting. At day 13, hypertrophic cardiomyopathy had progressed in severity and was treated with metoprolol. Echocardiography at age 2 months showed reduced biventricular function with severe ventricular hypertrophy. The size of the left ventricular posterior wall was 6–7 mm (*Z* score +5.3), and the left ventricular outflow tract was obstructed (V_{max} of 2.9 m/s). Although P1 was born with scalp hair, 8 weeks after birth, his scalp hair had been lost entirely (Figure 1). P1 deceased at the age of 3.5 months from severe hypertrophic cardiomyopathy.

Proband 2 (P2, Figure 1) is a male and the youngest child of healthy unrelated German parents. An elder brother is

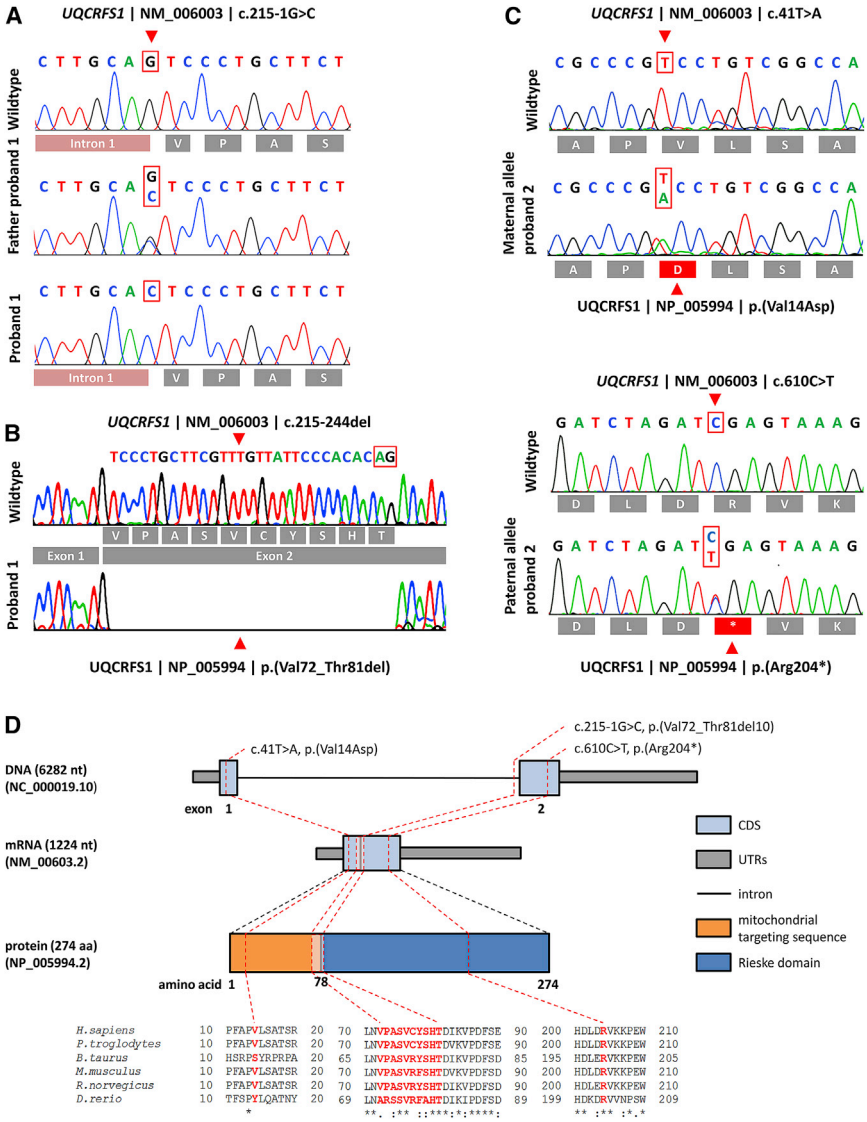

Figure 2. Molecular Genetic Findings in Both Probands

(A) Electropherograms of the homozygous c.215-1G>C splice-site variant in P1, which was heterozygous in both parents.

(B) Loss of the splice acceptor site of intron 1 leads to activation of an alternative downstream cryptic splice site (highlighted by a red box) with subsequent loss of 30 bp from the cDNA.

(C) Electropherograms of the compound heterozygous variants, c.41T>A inherited from the mother and c.610C>T from the father. The effect of the mutation on the amino acid sequence is depicted below the electropherograms.

(D) Genomic organization of *UQCRFS1* into two exons, the mRNA, and the protein structure depicting the location of the identified variants. The localization of the altered amino acids is highlighted on the protein domain structure. Phylogenetic conservation of the affected amino acid residues is presented in the alignment of homologs across different species. Positions of affected amino acids are highlighted in red. NB; the intronic region is not drawn to scale.

healthy. During pregnancy, fetal growth retardation and a persistent left upper *vena cava* were diagnosed. He was born at 37 weeks of gestation by *Caesarean* section due to fetal bradycardia. Postnatal complications arose from hypertrophic cardiomyopathy, ventricular septum defect (VSD), persistent fetal circulation, and lactic acidosis, as well as thrombocytopenia and severe normochromic anemia. During early infancy, feeding difficulties, muscular hypotonia, and a moderately delayed psychomotor development became evident. Febrile infections triggered a series of more than 10 severe metabolic crises with high lactate levels of up to 15 mmol/l (N 0.5–2.2). Under normal conditions, serum lactate levels were within the reference range. Cranial MRI performed at the ages of 6 months and 5 years did not reveal any abnormality, especially no signs for Leigh syndrome (Figure 1). Subsequently, the boy's condition stabilized, and he was able to walk independently at 23 months of age, while language and cognitive development were adequate for his age. Both VSD and persistent fetal circulation resolved spontaneously in the first year of life while the hypertrophic cardiomyopathy remained stable without impairment of cardiac function. Normocytic anemia with blood hemoglobin of 6.25 mmol/l (N 7.4–9.1) and thrombocytopenia with 178/nL (N 285–510) are persistent, but do not require therapeutic intervention. Assessment of cultured skin fibroblasts revealed isolated CIII deficiency (Table S3). At birth, P2 had very fine and curly hair of the scalp, which he lost entirely during early infancy. Since then, he has total alopecia of the scalp with very fine and sparse hair intermittently growing only to be lost again. In contrast, his eyelashes and eyebrows are present (Figure 1). Microscopic hair analysis did not reveal any abnormalities. At 5 years of age, bilateral papilledema was diagnosed despite normal cerebrospinal fluid pressure (13 cm H_2O) and without visual impairment. After initiation of Coenzyme Q_{10} supplementation with 8 mg/kg BW at the age of 6 years, the boy has remained in a good health for the last 3 years, without any further metabolic crises and with improved exercise tolerance. He displays slightly impaired gross and fine motor skills. His general muscle strength is reduced, but his walking ability in the plain is normal. The clinical phenotypes of both probands using the Human Phenotype Ontology[33] terms are described on Table 1.

In order to elucidate the genetic cause of the disease, we performed whole-exome sequencing (WES) on blood cell genomic DNA from both probands. This was done

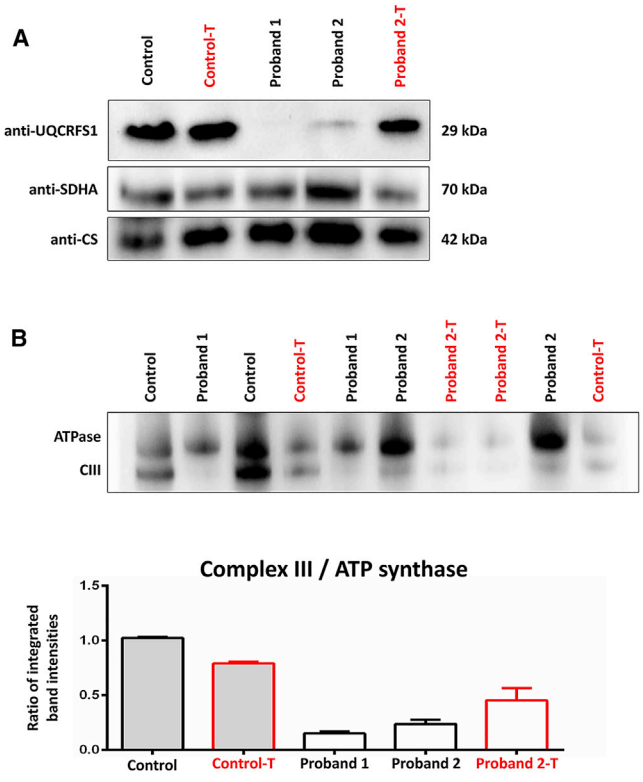

Figure 3. Protein Studies

(A) SDS-PAGE of fibroblast homogenates showing UQCRFS1 and SDHA. Citrate synthase (CS) was used as a mitochondrial loading control. UQCRFS1 protein levels were strongly reduced in P1 and P2 fibroblasts. Transduction rescued UQCRFS1 levels in P2 cells (Proband 2-T) and had no effect on control fibroblasts (Control-T). (B) BN-PAGE stained for ATP synthase and complex III (CIII) (using anti-ATP5F1A and anti-UQCRC2 antibodies) with densitometric analysis of CIII/ATP synthase ratios in BN-PAGE. Relative CIII reduction is rescued by lentiviral transduction in P2 fibroblasts. P1 fibroblasts reached a high passage number after transduction and did not replicate sufficiently enough to be included in this experiment. Bars depict the mean and SD of two repeated measurements.

independently at the Institute of Human Genetics, Technical University Munich and at the NeuroCure Clinical Research Center, Charité–Universitätsmedizin Berlin, as described.[34,35] Later, both groups connected via GeneMatcher.[36]

Clinical and biochemical data suggested a mitochondrial disorder with the autosomal recessive mode of inheritance. In P1, WES failed to identify likely pathogenic variants in genes associated with mitochondrial disease, but it did reveal a rare, potentially pathogenic homozygous splice-acceptor-site variant in *UQCRFS1* (chr19:g.29,699,066C>G [GRCh37.p11] | c.215-1G>C [RefSeq accession number NM_006003.2]; Figure 2) as the only mitochondrial protein candidate gene.[37] Segregation analysis via Sanger sequencing identified both parents as heterozygous carriers of this splice-site variant. To investigate the effect of this splice-site variant on the transcript level, we performed splicing analysis via RT-PCR and subsequent Sanger sequencing. This revealed a splicing defect resulting in the activation of a cryptic downstream splice-site and an in-frame deletion of 30 nucleotides and thus of 10 amino acids at a highly conserved region of the protein (Figure 2).

In P2, after assessing the pathogenic potential of variants with MutationTaster2,[38] we identified two heterozygous *UQCRFS1* variants (chr19:g.29,703,985A>T [GRCh37.p11] | c.41T>A [RefSeq NM_006003.2] | [p.Val14Asp] [RefSeq NP_005994.2] and chr19:g.29,698,670G>A | c.610C>T | [p.Arg204*]; Figure 2). Segregation analysis via Sanger sequencing showed the c.41T>A variant to be inherited from the mother and the c.610C>T variant from the father. His elder sibling was also tested and discovered to be heterozygous for the c.610C>T variant only. RT-PCR verified that the c.610C>T mutant transcript evaded nonsense-mediated mRNA messenger (NMD) decay (Figure S1) because the premature termination codon (PTC) was located within 3′ of the last exon-exon boundary.[39] No additional predicted pathogenic variants were detected for P2 in virtual gene panels for muscle diseases (n = 337 genes) and alopecia (n = 62 genes) (see Supplemental Information). Bioinformatic analysis of p.Val14Asp on the TargetP-2.0 Server[40] showed that replacement of the non-polar valine by a negatively charged aspartic acid in the MTS reduces the probability that the MTS will fold correctly into an amphiphilic α-helix.[41] All identified *UQCRFS1* variants were submitted to ClinVar (see Accession Numbers). They affect regions that are highly conserved across vertebrates (Figure 2) and have neither been reported in public databases (gnomAD) nor in our in-house database, which contains >16,000 exome datasets of individuals with unrelated phenotypes.

In order to characterize the consequence of the *UQCRFS1* variants, we did functional investigations on primary fibroblast cell lines from both probands. Proband and control fibroblasts were cultivated in DMEM media supplemented with 10% FBS, 1% penicillin-streptomycin, and 200 μmol/l uridine at 37°C and 5% CO_2. First, we assessed steady-state levels of UQCRFS1 protein by SDS-PAGE of fibroblast cell lysates. Immunoblotting using antibodies against UQCRFS1 (1:1,000, Abcam, ab14746), SDHA (1:3,000, Abcam, ab14715, a subunit of CII, the only respiratory chain complex not involved in the supercomplexes), and citrate synthase (CS) (1:3,000; THP, NBP2-43648) as controls for mitochondrial proteins showed strongly reduced UQCRFS1 band intensities in both probands, and hardly any signal was detected in P1 (Figure 3). Next, we wanted to gain insight into the consequences of UQCRFS1 depletion on CIII composition. To do this, we separated multi-protein complexes from lauryl-maltoside-solubilized fibroblast mitochondria in their native conformation through the use of Blue Native Polyacrylamide Gel Electrophoresis (BN-PAGE).[25] In accordance with the crucial role of UQCRFS1 in CIII assembly and function, after we stained for $CIII_2$ (UQCRC2; 1:1,500; Abcam, ab14745) and ATP synthase (ATP5F1A; 1:2,000; Abcam, ab14748) as control, assembled $CIII_2$ was barely detectable in both probands' mitochondria (Figure 3). $CIII_2$ depletion indicated impaired

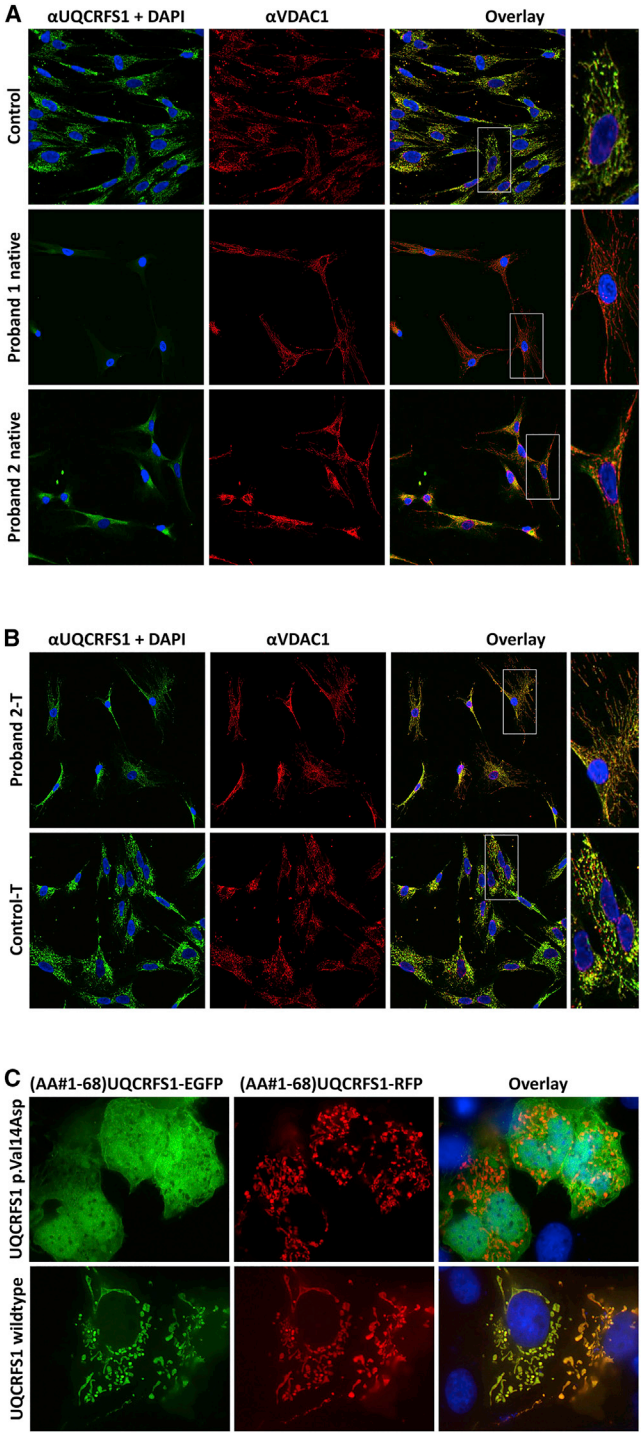

Figure 4. Immunohistology and Mitochondrial Import
(A) Absent or reduced UQCRFS1 protein levels in both probands' fibroblasts in comparison to wild-type (WT) control fibroblasts. The anti-VDAC1 antibody signal marks the mitochondria. In WT fibroblasts, anti-UQCRFS1 and anti-VDAC1 signals colocalized, thereby verifying the mitochondrial localization of UQCRFS1 (see magnified inset on the right). Nuclei stained with DAPI.
(B) Lentiviral transduction of UQCRFS1 in the fibroblasts of P2 (Proband 2-T) restores normal localization.
(C) The first 68 amino acids of WT and p.Val14Asp mutant mitochondrial import sequences of UQCRFS1 were fused to the enhanced green fluorescent protein (EGFP). For control, the WT sequence was fused to red fluorescent protein (RFP). After co-transfection of EGFP and RFP constructs into COS1 cells, only those EGFP constructs were imported into the mitochondria that carried the WT import sequence. The p.Val14Asp variant entirely prevented mitochondrial import.

oxidative phosphorylation, which was later confirmed via microscale respirometry (Seahorse) in both fibroblast cell lines.[42]

In order to investigate the subcellular distribution of wild-type (WT) and mutant UQCRFS1, we immunostained control and proband fibroblasts with anti-UQCRFS1 (1:100, Abcam, ab14746) and anti-VDAC1 (1:400, Abcam, ab15895) antibodies. The results confirmed a strong reduction of UQCRFS1 protein abundance in the mitochondria of both probands (Figure 4). For verification of the mitochondrial import defect caused by the *UQCRFS1* c.41T>A variant, we cloned a set of protein expression plasmids by fusing the 5′ 204 bp of the WT and c.41T>A mutant *UQCRFS2* cDNA (encoding the 68 N-terminal amino acids) to the coding sequence of EGFP (p.Val14-EGFP and p.Asp14-EGFP constructs). For controls, we fused the WT sequence to an RFP sequence (p.Val14-RFP construct). We transfected a mixture of p.Val14-EGFP + p.Val14-RFP and of p.Asp14-EGFP + p.Val14-RFP constructs into COS1 cells, and we followed the distributions of the fusion proteins through the use of fluorescence microscopy. The WT red and green fusion proteins had a normal mitochondrial distribution, while the mutant fusion protein failed to be imported and was found to be distributed over the entire cytosol and in the nucleus (Figure 4).

In order to determine whether the identified *UQCRFS1* variants are indeed responsible for the CIII defect, we tested whether a WT copy of the *UQCRFS1* cDNA could rescue the CIII deficiency in proband fibroblasts after lentiviral transduction.[43] Only P2-transduced cells were growing sufficiently well to generate enough material to verify the rescue of all the various phenotypes; later, the growth potential these fibroblasts was also exhausted, which only allowed two repetitions of the experiment with comparative low cellular yields. Functional analysis confirmed that the transduction of cell lines with a WT *UQCRFS1* cDNA transcript restored normal UQCRFS1 levels in P2 (Figure 3), restored the CIII assembly defect in P2 (Figure 3), and rescued the respiration defect in both probands' cell lines (Figure 5 and Figures S2–S4). The Seahorse protocol allows calculation of various parameters pertinent to mitochondrial function (Figure S5). These show significant improvement of basal respiration, ATP production, maximum respiration, and spare respiratory capacity after lentiviral transduction. The maximum respiration could be augmented into the normal range (Figure S5).

Because P2 had clinically benefitted from Coenzyme Q_{10} supplementation, we incubated his fibroblasts for 7 h in 0, 10, 30, and 100 μM Coenzyme Q_{10} prior to measurement of CIII activity and oxygen consumption rate, but we did not find any significant differences in the ensuing oxygen consumption rates (Figure S6).

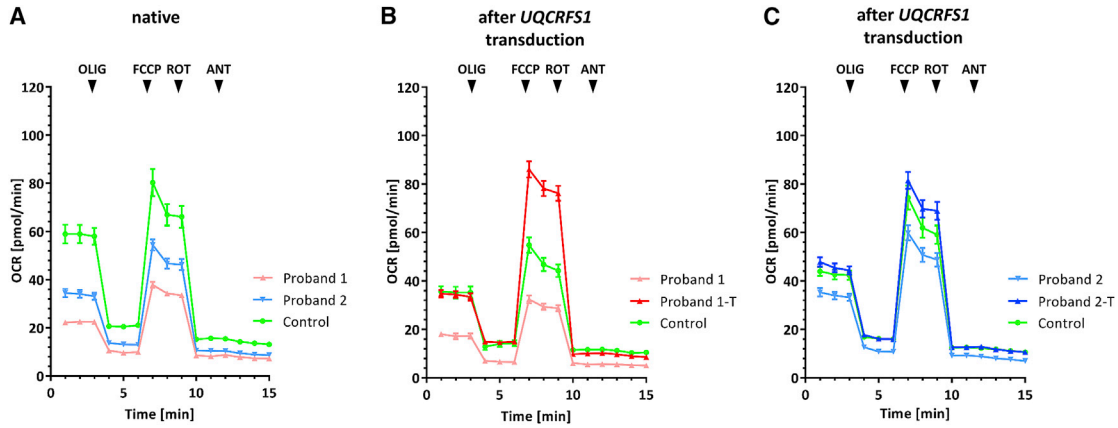

Figure 5. Microscale Respirometry Analysis in Fibroblasts
Combination of two replication experiments of normalized oxygen consumption rates (OCRs) of proband and control fibroblasts as measured with the Seahorse instrument (two biological replicates, 12–16 technical replicates for each condition). Each data point represents mean ± SEMs of measurements from 24–32 wells of technical replicates. The separate replication experiments are depicted in Figures S2–S4. OLIG, oligomycin; FCCP, carbonyl cyanide m-chlorophenyl hydrazone; ROT, rotenone; ANT; antimycine.
(A) Oxygen consumption rates of fibroblasts in the native state.
(B) Rescue of the OCR in fibroblasts of proband P1 after transduction with a lentivirus encoding wild-type (WT) *UQCRFS1* (Proband 1-T).
(C) Rescue of the OCR of fibroblasts of P2 after transduction with a lentivirus encoding WT *UQCRFS1* (Proband 2-T). NB, we normalized the OCRs of different wells in the Seahorse experiment separately for each plate. For that, we first determined cell numbers in each well through the use of the CyQUANT kit (ThermoFischer) and computed a correction factor for each well by dividing the number of cells in the individual well by the average number of cells in the wells of the whole plate. For normalization of OCR values, we then divided raw OCR readings from each well by its correction factor.

Mitochondrial diseases associated with isolated CIII deficiency are rare, and due to general technical difficulties in measuring CIII activity in human tissues, they might be underdiagnosed.[44] They may also be missed due to unremarkable or statistically insignificant reduction of CIII activity in the tissues under investigation. The increasing application of WES and whole-genome sequencing early in the diagnostic work-up will provide a more unbiased picture about the frequency of CIII deficiencies in the future.[45]

Considering the crucial role of UQCRFS1 for the catalytic function of CIII, it was no surprise that homozygous *Uqcrfs1* loss-of-function variants are embryonically lethal in mice,[46] and variants associated with impaired UQCRFS1 function are disease-causing. Here we describe two probands with pathogenic bi-allelic variants in *UQCRFS1* leading to CIII deficiency. Their shared clinical features included fetal bradycardia, lactic acidosis, thrombocytopenia, hypertrophic cardiomyopathy, and *alopecia totalis*. It is estimated that cardiomyopathy occurs in 20%–40% of children with mitochondrial disorders, and hypertrophic cardiomyopathy is the most frequently observed of these cardiac manifestations.[47,48] Hypertrophic cardiomyopathy was observed in two individuals with *BCS1L* variants.[49] In addition, different forms of cardiomyopathy (hypertrophic, dilated, and histiocytoid) have been described in three individuals with *MT-CYB* variants.[19,50,51] In one instance, the *MT-CYB* variant m.15243G>A (p.Gly166Glu) (RefSeq NC_012920.1) from an individual with cardiomyopathy[50] disrupted the interaction between cytochrome b and UQCRFS1 in a yeast model of the disease.[52]

Early onset *alopecia totalis* is rarely observed in individuals with mitochondrial disease. In the past, 14 individuals were reported with specific hair and skin disorders in a group of 140 children with mitochondrial diseases, and three of those were CIII deficient.[53] In addition, *pili torti* and secondary *alopecia* are common hair abnormalities of *BSC1L*-related Björnstad syndrome.[29] Besides the above mentioned features, P2 suffers from chronic anemia and both probands suffered from thrombocytopenia, which is a known feature of mitochondrial disorders, especially of Pearson's syndrome.[54] Recent investigations in mice elucidated the importance of the Rieske iron-sulfur protein (RISP) and overall CIII function in hematopoiesis and immune response. Cell-specific loss of RISP in fetal hematopoietic stem cells impaired their differentiation, resulting in anemia and prenatal death.[55] Cell-specific *Uqcrfs1* knockout in regulatory T cells in mice led to an early-onset fatal inflammatory disease without any effect on the number of regulatory T cells. This suggests a role of CIII in the modulation of protein products relevant for regulation and suppression of immune responses.[56]

In summary, we have expanded the clinical and mutational spectrum of CIII deficiencies by reporting pathogenic variants in *UQCRFS1* that lead to a mitochondrial disorder in two unrelated individuals. Persistent clinical improvement of individual P2 after high-dosage Coenzyme Q_{10} supplementation points toward a therapeutic option despite the fact that we did not see any increase in the oxygen consumption rate in his fibroblasts. Such supplementation might be beneficial if some residual CIII activity is present, but more research has to be done

regarding the pharmacokinetics, subcellular distribution, and effect of Coenzyme Q_{10} supplementation.

Accession Numbers

The accession numbers for the data reported in this paper are:

- For proband 1, c.215-1G>C, ClinVar: VCV000619297, and
- For proband 2, c.41T>A, ClinVar: VCV000619501 and c.610C>T, ClinVar: VCV000619499

Supplemental Data

Supplemental Data can be found online at https://doi.org/10.1016/j.ajhg.2019.12.005.

Acknowledgments

The authors thank the families for participation in the study. The project was funded by the German Research Foundation und Germany's Excellence Strategy (EXC-2049—390688087) to M.S.; the E-Rare project GENOMIT (01GM1603 and 01GM1207 to H.P. and O1GML1207 to A.R.); the German network for mitochondrial disorders, MitoNET, (01GM1996B) to H.P.; and the Austrian Science Funds (FWF, I 2741-B26) to J.A.M. A Fellowship through the Graduate School of Quantitative Biosciences Munich (QBM) supports V.A.Y.

Declaration of Interests

The authors declare no competing interests.

Received: July 16, 2019
Accepted: December 5, 2019
Published: December 26, 2019

Web Resources

ClinVar, https://www.ncbi.nlm.nih.gov/clinvar/
ExAC Browser, http://exac.broadinstitute.org/
GenBank, https://www.ncbi.nlm.nih.gov/genbank/
GeneMatcher, https://www.genematcher.org
gnomAD Browser, https://gnomad.broadinstitute.org/
MutationTaster2, http://www.mutationtaster.org/
OMIM, https://www.omim.org/
TargetP-2.0 Server, http://www.cbs.dtu.dk/services/TargetP/

References

1. Crofts, A.R., Holland, J.T., Victoria, D., Kolling, D.R.J., Dikanov, S.A., Gilbreth, R., Lhee, S., Kuras, R., and Kuras, M.G. (2008). The Q-cycle reviewed: How well does a monomeric mechanism of the bc(1) complex account for the function of a dimeric complex? Biochim. Biophys. Acta *1777*, 1001–1019.
2. Iwata, S., Lee, J.W., Okada, K., Lee, J.K., Iwata, M., Rasmussen, B., Link, T.A., Ramaswamy, S., and Jap, B.K. (1998). Complete structure of the 11-subunit bovine mitochondrial cytochrome bc1 complex. Science *281*, 64–71.
3. Xia, D., Esser, L., Tang, W.-K., Zhou, F., Zhou, Y., Yu, L., and Yu, C.-A. (2013). Structural analysis of cytochrome bc1 complexes: implications to the mechanism of function. Biochim. Biophys. Acta *1827*, 1278–1294.
4. Smith, P.M., Fox, J.L., and Winge, D.R. (2012). Reprint of: Biogenesis of the cytochrome bc(1) complex and role of assembly factors. Biochim. Biophys. Acta *1817*, 872–882.
5. Sánchez, E., Lobo, T., Fox, J.L., Zeviani, M., Winge, D.R., and Fernández-Vizarra, E. (2013). LYRM7/MZM1L is a UQCRFS1 chaperone involved in the last steps of mitochondrial Complex III assembly in human cells. Biochim. Biophys. Acta *1827*, 285–293.
6. Invernizzi, F., Tigano, M., Dallabona, C., Donnini, C., Ferrero, I., Cremonte, M., Ghezzi, D., Lamperti, C., and Zeviani, M. (2013). A homozygous mutation in LYRM7/MZM1L associated with early onset encephalopathy, lactic acidosis, and severe reduction of mitochondrial complex III activity. Hum. Mutat. *34*, 1619–1622.
7. Maio, N., Kim, K.S., Singh, A., and Rouault, T.A. (2017). A Single Adaptable Cochaperone-Scaffold Complex Delivers Nascent Iron-Sulfur Clusters to Mammalian Respiratory Chain Complexes I-III. Cell Metab. *25*, 945–953.e6.
8. Nobrega, F.G., Nobrega, M.P., and Tzagoloff, A. (1992). BCS1, a novel gene required for the expression of functional Rieske iron-sulfur protein in Saccharomyces cerevisiae. EMBO J. *11*, 3821–3829.
9. Fernandez-Vizarra, E., and Zeviani, M. (2018). Mitochondrial complex III Rieske Fe-S protein processing and assembly. Cell Cycle *17*, 681–687.
10. Brandt, U., Yu, L., Yu, C.A., and Trumpower, B.L. (1993). The mitochondrial targeting presequence of the Rieske iron-sulfur protein is processed in a single step after insertion into the cytochrome bc1 complex in mammals and retained as a subunit in the complex. J. Biol. Chem. *268*, 8387–8390.
11. Bottani, E., Cerutti, R., Harbour, M.E., Ravaglia, S., Dogan, S.A., Giordano, C., Fearnley, I.M., D'Amati, G., Viscomi, C., Fernandez-Vizarra, E., and Zeviani, M. (2017). TTC19 Plays a Husbandry Role on UQCRFS1 Turnover in the Biogenesis of Mitochondrial Respiratory Complex III. Mol. Cell *67*, 96–105.e4.
12. Gu, J., Wu, M., Guo, R., Yan, K., Lei, J., Gao, N., and Yang, M. (2016). The architecture of the mammalian respirasome. Nature *537*, 639–643.
13. Letts, J.A., Fiedorczuk, K., and Sazanov, L.A. (2016). The architecture of respiratory supercomplexes. Nature *537*, 644–648.
14. Wu, M., Gu, J., Guo, R., Huang, Y., and Yang, M. (2016). Structure of Mammalian Respiratory Supercomplex $I_1III_2IV_1$. Cell *167*, 1598–1609.e10.
15. Bénit, P., Lebon, S., and Rustin, P. (2009). Respiratory-chain diseases related to complex III deficiency. Biochim. Biophys. Acta *1793*, 181–185.
16. Meunier, B., Fisher, N., Ransac, S., Mazat, J.-P., and Brasseur, G. (2013). Respiratory complex III dysfunction in humans and the use of yeast as a model organism to study mitochondrial myopathy and associated diseases. Biochim. Biophys. Acta *1827*, 1346–1361.
17. Fernández-Vizarra, E., and Zeviani, M. (2015). Nuclear gene mutations as the cause of mitochondrial complex III deficiency. Front. Genet. *6*, 134.
18. Andreu, A.L., Hanna, M.G., Reichmann, H., Bruno, C., Penn, A.S., Tanji, K., Pallotti, F., Iwata, S., Bonilla, E., Lach, B., et al. (1999). Exercise intolerance due to mutations in the cytochrome b gene of mitochondrial DNA. N. Engl. J. Med. *341*, 1037–1044.
19. Schuelke, M., Krude, H., Finckh, B., Mayatepek, E., Janssen, A., Schmelz, M., Trefz, F., Trijbels, F., and Smeitink, J. (2002).

Septo-optic dysplasia associated with a new mitochondrial cytochrome b mutation. Ann. Neurol. *51*, 388–392.
20. Gaignard, P., Menezes, M., Schiff, M., Bayot, A., Rak, M., Ogier de Baulny, H., Su, C.-H., Gilleron, M., Lombes, A., Abida, H., et al. (2013). Mutations in CYC1, encoding cytochrome c1 subunit of respiratory chain complex III, cause insulin-responsive hyperglycemia. Am. J. Hum. Genet. *93*, 384–389.
21. Miyake, N., Yano, S., Sakai, C., Hatakeyama, H., Matsushima, Y., Shiina, M., Watanabe, Y., Bartley, J., Abdenur, J.E., Wang, R.Y., et al. (2013). Mitochondrial complex III deficiency caused by a homozygous UQCRC2 mutation presenting with neonatal-onset recurrent metabolic decompensation. Hum. Mutat. *34*, 446–452.
22. Haut, S., Brivet, M., Touati, G., Rustin, P., Lebon, S., Garcia-Cazorla, A., Saudubray, J.M., Boutron, A., Legrand, A., and Slama, A. (2003). A deletion in the human QP-C gene causes a complex III deficiency resulting in hypoglycaemia and lactic acidosis. Hum. Genet. *113*, 118–122.
23. Barel, O., Shorer, Z., Flusser, H., Ofir, R., Narkis, G., Finer, G., Shalev, H., Nasasra, A., Saada, A., and Birk, O.S. (2008). Mitochondrial complex III deficiency associated with a homozygous mutation in UQCRQ. Am. J. Hum. Genet. *82*, 1211–1216.
24. Tucker, E.J., Wanschers, B.F.J., Szklarczyk, R., Mountford, H.S., Wijeyeratne, X.W., van den Brand, M.A.M., Leenders, A.M., Rodenburg, R.J., Reljić, B., Compton, A.G., et al. (2013). Mutations in the UQCC1-interacting protein, UQCC2, cause human complex III deficiency associated with perturbed cytochrome b protein expression. PLoS Genet. *9*, e1004034.
25. Feichtinger, R.G., Brunner-Krainz, M., Alhaddad, B., Wortmann, S.B., Kovacs-Nagy, R., Stojakovic, T., Erwa, W., Resch, B., Windischhofer, W., Verheyen, S., et al. (2017). Combined Respiratory Chain Deficiency and *UQCC2* Mutations in Neonatal Encephalomyopathy: Defective Supercomplex Assembly in Complex III Deficiencies. Oxid. Med. Cell. Longev. *2017*, 7202589.
26. Wanschers, B.F.J., Szklarczyk, R., van den Brand, M.A.M., Jonckheere, A., Suijskens, J., Smeets, R., Rodenburg, R.J., Stephan, K., Helland, I.B., Elkamil, A., et al. (2014). A mutation in the human CBP4 ortholog UQCC3 impairs complex III assembly, activity and cytochrome b stability. Hum. Mol. Genet. *23*, 6356–6365.
27. de Lonlay, P., Valnot, I., Barrientos, A., Gorbatyuk, M., Tzagoloff, A., Taanman, J.W., Benayoun, E., Chrétien, D., Kadhom, N., Lombès, A., et al. (2001). A mutant mitochondrial respiratory chain assembly protein causes complex III deficiency in patients with tubulopathy, encephalopathy and liver failure. Nat. Genet. *29*, 57–60.
28. Visapää, I., Fellman, V., Vesa, J., Dasvarma, A., Hutton, J.L., Kumar, V., Payne, G.S., Makarow, M., Van Coster, R., Taylor, R.W., et al. (2002). GRACILE syndrome, a lethal metabolic disorder with iron overload, is caused by a point mutation in BCS1L. Am. J. Hum. Genet. *71*, 863–876.
29. Hinson, J.T., Fantin, V.R., Schönberger, J., Breivik, N., Siem, G., McDonough, B., Sharma, P., Keogh, I., Godinho, R., Santos, F., et al. (2007). Missense mutations in the BCS1L gene as a cause of the Björnstad syndrome. N. Engl. J. Med. *356*, 809–819.
30. Ghezzi, D., Arzuffi, P., Zordan, M., Da Re, C., Lamperti, C., Benna, C., D'Adamo, P., Diodato, D., Costa, R., Mariotti, C., et al. (2011). Mutations in TTC19 cause mitochondrial complex III deficiency and neurological impairment in humans and flies. Nat. Genet. *43*, 259–263.
31. Morán, M., Marín-Buera, L., Gil-Borlado, M.C., Rivera, H., Blázquez, A., Seneca, S., Vázquez-López, M., Arenas, J., Martín, M.A., and Ugalde, C. (2010). Cellular pathophysiological consequences of BCS1L mutations in mitochondrial complex III enzyme deficiency. Hum. Mutat. *31*, 930–941.
32. Ghezzi, D., and Zeviani, M. (2018). Human diseases associated with defects in assembly of OXPHOS complexes. Essays Biochem. *62*, 271–286.
33. Groza, T., Köhler, S., Moldenhauer, D., Vasilevsky, N., Baynam, G., Zemojtel, T., Schriml, L.M., Kibbe, W.A., Schofield, P.N., Beck, T., et al. (2015). The Human Phenotype Ontology: Semantic Unification of Common and Rare Disease. Am. J. Hum. Genet. *97*, 111–124.
34. Schottmann, G., Seelow, D., Seifert, F., Morales-Gonzalez, S., Gill, E., von Au, K., von Moers, A., Stenzel, W., and Schuelke, M. (2015). Recessive REEP1 mutation is associated with congenital axonal neuropathy and diaphragmatic palsy. Neurol. Genet. *1*, e32.
35. Kremer, L.S., Bader, D.M., Mertes, C., Kopajtich, R., Pichler, G., Iuso, A., Haack, T.B., Graf, E., Schwarzmayr, T., Terrile, C., et al. (2017). Genetic diagnosis of Mendelian disorders via RNA sequencing. Nat. Commun. *8*, 15824.
36. Sobreira, N., Schiettecatte, F., Valle, D., and Hamosh, A. (2015). GeneMatcher: a matching tool for connecting investigators with an interest in the same gene. Hum. Mutat. *36*, 928–930.
37. Elstner, M., Andreoli, C., Klopstock, T., Meitinger, T., and Prokisch, H. (2009). Chapter 1: The Mitochondrial Proteome Database: MitoP2. In Methods in Enzymology (Academic Press), pp. 3–20.
38. Schwarz, J.M., Cooper, D.N., Schuelke, M., and Seelow, D. (2014). MutationTaster2: mutation prediction for the deep-sequencing age. Nat. Methods *11*, 361–362.
39. Thermann, R., Neu-Yilik, G., Deters, A., Frede, U., Wehr, K., Hagemeier, C., Hentze, M.W., and Kulozik, A.E. (1998). Binary specification of nonsense codons by splicing and cytoplasmic translation. EMBO J. *17*, 3484–3494.
40. Emanuelsson, O., Brunak, S., von Heijne, G., and Nielsen, H. (2007). Locating proteins in the cell using TargetP, SignalP and related tools. Nat. Protoc. *2*, 953–971.
41. von Heijne, G., Steppuhn, J., and Herrmann, R.G. (1989). Domain structure of mitochondrial and chloroplast targeting peptides. Eur. J. Biochem. *180*, 535–545.
42. Yépez, V.A., Kremer, L.S., Iuso, A., Gusic, M., Kopajtich, R., Koňaříková, E., Nadel, A., Wachutka, L., Prokisch, H., and Gagneur, J. (2018). OCR-Stats: Robust estimation and statistical testing of mitochondrial respiration activities using Seahorse XF Analyzer. PLoS ONE *13*, e0199938.
43. Kremer, L.S., and Prokisch, H. (2017). Identification of disease-causing mutations by functional complementation of patient-derived fibroblast cell lines. In Mitochondria: Practical Protocols, D. Mokranjac and F. Perocchi, eds. (New York, NY: Springer New York), pp. 391–406.
44. Chretien, D., Slama, A., Brière, J.-J., Munnich, A., Rötig, A., and Rustin, P. (2004). Revisiting pitfalls, problems and tentative solutions for assaying mitochondrial respiratory chain complex III in human samples. Curr. Med. Chem. *11*, 233–239.
45. Stenton, S.L., and Prokisch, H. (2018). Advancing genomic approaches to the molecular diagnosis of mitochondrial disease. Essays Biochem. *62*, 399–408.
46. Hughes, B.G., and Hekimi, S. (2011). A mild impairment of mitochondrial electron transport has sex-specific effects on lifespan and aging in mice. PLoS ONE *6*, e26116.

47. Scaglia, F., Towbin, J.A., Craigen, W.J., Belmont, J.W., Smith, E.O., Neish, S.R., Ware, S.M., Hunter, J.V., Fernbach, S.D., Vladutiu, G.D., et al. (2004). Clinical spectrum, morbidity, and mortality in 113 pediatric patients with mitochondrial disease. Pediatrics *114*, 925–931.
48. Yaplito-Lee, J., Weintraub, R., Jamsen, K., Chow, C.W., Thorburn, D.R., and Boneh, A. (2007). Cardiac manifestations in oxidative phosphorylation disorders of childhood. J. Pediatr. *150*, 407–411.
49. Al-Owain, M., Colak, D., Albakheet, A., Al-Younes, B., Al-Humaidi, Z., Al-Sayed, M., Al-Hindi, H., Al-Sugair, A., Al-Muhaideb, A., Rahbeeni, Z., et al. (2013). Clinical and biochemical features associated with BCS1L mutation. J. Inherit. Metab. Dis. *36*, 813–820.
50. Valnot, I., Kassis, J., Chretien, D., de Lonlay, P., Parfait, B., Munnich, A., Kachaner, J., Rustin, P., and Rötig, A. (1999). A mitochondrial cytochrome b mutation but no mutations of nuclearly encoded subunits in ubiquinol cytochrome c reductase (complex III) deficiency. Hum. Genet. *104*, 460–466.
51. Hagen, C.M., Aidt, F.H., Havndrup, O., Hedley, P.L., Jespersgaard, C., Jensen, M., Kanters, J.K., Moolman-Smook, J.C., Møller, D.V., Bundgaard, H., and Christiansen, M. (2013). MT-CYB mutations in hypertrophic cardiomyopathy. Mol. Genet. Genomic Med. *1*, 54–65.
52. Fisher, N., Bourges, I., Hill, P., Brasseur, G., and Meunier, B. (2004). Disruption of the interaction between the Rieske iron-sulfur protein and cytochrome b in the yeast bc1 complex owing to a human disease-associated mutation within cytochrome b. Eur. J. Biochem. *271*, 1292–1298.
53. Bodemer, C., Rötig, A., Rustin, P., Cormier, V., Niaudet, P., Saudubray, J.-M., Rabier, D., Munnich, A., and de Prost, Y. (1999). Hair and skin disorders as signs of mitochondrial disease. Pediatrics *103*, 428–433.
54. Finsterer, J. (2007). Hematological manifestations of primary mitochondrial disorders. Acta Haematol. *118*, 88–98.
55. Ansó, E., Weinberg, S.E., Diebold, L.P., Thompson, B.J., Malinge, S., Schumacker, P.T., Liu, X., Zhang, Y., Shao, Z., Steadman, M., et al. (2017). The mitochondrial respiratory chain is essential for haematopoietic stem cell function. Nat. Cell Biol. *19*, 614–625.
56. Weinberg, S.E., Singer, B.D., Steinert, E.M., Martinez, C.A., Mehta, M.M., Martínez-Reyes, I., Gao, P., Helmin, K.A., Abdala-Valencia, H., Sena, L.A., et al. (2019). Mitochondrial complex III is essential for suppressive function of regulatory T cells. Nature *565*, 495–499.